Inorg. Chem. **2003**, *42*, 3047–3056

Minor Groove Site Coordination of Adenine by Platinum Group Metal Ions: Effects on Basicity, Base Pairing, and Electronic Structure

David Amantia, Clayton Price, Michelle A. Shipman, Mark R. J. Elsegood, William Clegg, and Andrew Houlton*

School of Natural Sciences: Chemistry, University of Newcastle upon Tyne, Newcastle upon Tyne, NE1 7RU, U.K.

Received November 5, 2002

Dithioether- or diamine-tethered adenine derivatives react with Pt^{II}, Pd^{II}, and Rh^{III} ions to give N3-coordinated complexes of the types $[MCl(SSN)]^+$ (M = Pt or Pd), $[RhCl_3(SSN)]$, or $[RhCl_3(NNN)]$ (where SSN = 1-(N9-adenine)-3,6-dithia-heptane or 1-(N9-adenine)-4,7-dithia-octane; NNN = ethylenediamine-*N*,9-ethyladenine). Single-crystal X-ray analysis confirms the nature of the metal–nucleobase interaction and highlights a conserved intermolecular hydrogen-bonding motif for all the complexes, irrespective of the metal-ion geometry. Coordination significantly reduces the basicity of the adeninyl group, as indicated by a pK_a value of –0.16 for [PtCl(N3-1-(N9-adenine)-3,6-dithia-heptane)]BF_4, compared to a pK_a value of 4.2 for 9-ethyladenine. The site of proton binding, N1 or N7, could not be unambiguously assigned from the ^{1}H NMR data, because of the similar effect on the chemical shifts of the H2 and H8 protons. Density functional calculations at the BP-LACVP* level suggest N1 as the site of protonation for this type of complex. This is in contrast to the N7-protonation reported for [Pt(dien)(N3-6,6′,9-trimethyladenine)]$^{2+}$, as reported elsewhere (Meiser et al., *Chem.—Eur. J.* **1997**, *3*, 388). *However, further electronic structure calculations in the gas phase reveal that the preferred site for protonation for N3-bound complexes is conformationally dependent.* N3 coordination was also found to reduce the extent of base pairing between adenine and thymine in dimethylsulfoxide for the self-complementary complex [PtCl(**L3**)]$^+$ (**L3** = 1-(N9-adenine)-3,6-dithia-9-(N1-thymine)nonane), compared to that for the uncomplexed ligand.

Introduction

The interaction of metal ions and complexes with nucleic acids and their constituents is of central importance to many aspects of their structure and function.[1,2] Much of our understanding of this has been obtained from studies on model systems.[3,4] In addition to identifying preferred sites for coordination, small-molecule experimental[5−8] and theoretical[9,10] models have been used to investigate the effect of metal-ion binding on the stability and structure of base pairs. Metal-ion stabilization of rare tautomeric forms that possess different, and, thus, potentially mutagenic, hydrogen-bonding patterns have also been identified in this way.[10−15]

The majority of these examples are concerned with coordination at the sites located in the major groove of duplex DNA. However, an increasing number of studies highlight interactions between metal ions and sites that are located in

* Author to whom correspondence should be addressed. E-mail: Andrew.Houlton@ncl.ac.uk.

(1) Sigel, A., Sigel, H., Eds. *Interactions of Metal Ions with Nucleotides, Nucleic Acids and Their Constituents*; Marcel Dekker: New York, 1996; Vol. 32.
(2) Sigel, A., Sigel, H., Eds. *Probing of Nucleic Acids by Metal Ion Complexes of Small Molecules*; Marcel Dekker: New York, 1996; Vol. 33.
(3) Lippert, B. *Coord. Chem. Rev.* **2000**, *200−202*, 487.
(4) Sigel, A.; Sigel, H. *Met. Ions Biol. Syst.* **1996**, *33*, 678.
(5) Sigel, R. K. O.; Lippert, B. *Chem. Commun.* **1999**, 2167.
(6) Sigel, R. K. O.; Freisinger, E.; Lippert, B. *J. Biol. Inorg. Chem.* **2000**, *5*, 287.
(7) Bruning, W.; Sigel, R. K. O.; Freisinger, E.; Lippert, B. *Angew. Chem., Int. Ed.* **2001**, *40*, 3397.
(8) Luth, M. S.; Freisinger, E.; Lippert, B. *Chem.—Eur. J.* **2001**, *7*, 2104.
(9) Šponer, J.; Sabat, M.; Burda, J. V.; Doody, A. M.; Leszczynski, J.; Hobza, P. *J. Biomol. Struct. Dyn.* **1998**, *16*, 139.
(10) Šponer, J.; Šponer, J. E.; Gorb, L.; Leszczynski, J.; Lippert, B. *J. Phys. Chem. A* **1999**, *103*, 11406.
(11) Pichierri, F.; Holthenrich, D.; Zangrando, E.; Lippert, B.; Randaccio, L. *J. Biol. Inorg. Chem.* **1996**, *1*, 439.
(12) Zamora, F.; Kunsman, M.; Sabat, M.; Lippert, B. *Inorg. Chem.* **1997**, *36*, 1583.
(13) Muller, J.; Zangrando, E.; Pahlke, N.; Freisinger, E.; Randaccio, L.; Lippert, B. *Chem.—Eur. J.* **1998**, *4*, 397.
(14) Muller, J.; Sigel, R. K. O.; Lippert, B. *J. Inorg. Biochem.* **2000**, *79*, 261.
(15) Velders, A. H.; van der Geest, B.; Kooijman, H.; Spek, A. L.; Haasnoot, J. G.; Reedijk, J. *Eur. J. Inorg. Chem.* **2001**, 369.

10.1021/ic020657g CCC: $25.00
Published on Web 04/04/2003

the minor groove.[16−27] Specific examples include alkali-metal ions, which appear to show critical sequence dependence,[17,24] whereas divalent d-block ions have been shown to localize at A-tracts in dodecamer duplex DNA.[18] Rh^{III}−N3 binding has been proposed for the product of the photolysis reaction between *cis*-$Rh(phen)_2Cl_2$ and deoxyadenosine,[28] and, more recently, Sletten et al. reported an A−N3:G−N7 intrastrand adduct formed by a potent *trans*-platinum antitumor agent.[29]

The rational synthesis of nucleobase complexes that feature coordination at rare binding sites, such as those located in the minor groove, is not well developed.[27] Synthetic strategies for preparing N3-coordinated adenine complexes rely upon some method for inhibiting N1/N7 binding. Steric hindrance has been used to block binding at N1 or N7 by alkylating the exocyclic amino group, N6.[20,21,30,31] Such substitution does, however, preclude studies on the effect of coordination on the hydrogen bonding. Loeb et al. showed that second-sphere binding may also induce N3−A binding.[19,32] We have been using chelate-tethered nucleobase derivatives as a means of probing the reactivity of the N3 site of A and G nucleobases (Chart 1).[33−39] Previously, the chelating group used has generally been ethylenediamine; here, we extend this to thioether strands. The rationales for developing such strands were twofold. First, competitive hydrogen-bonding sites are removed from the chelating tether, compared to the previous diamine analogues. This maximizes the formation of internucleobase hydrogen-bonding interactions. Second,

Chart 1. Comparison of Adenine (Left) with a Chelate-Tethered Analogue Used To Enhance Binding to N3 (n = 1 or 2, and D = NH/NH_2 or S/S-Me)

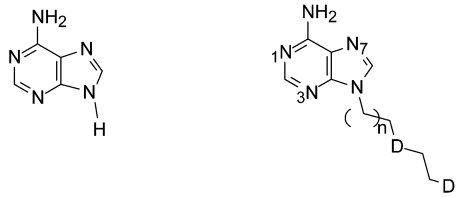

to date, our attempts to prepare Pt^{II} complexes have been rather unsuccessful, principally because of, we suspect, the formation of polynuclear aggregates and oligomers. In this work, we have prepared dithioether derivatives of N9-alkyladenine and structurally characterized a series of N3-coordinated derivatives containing Pt^{II}, Pd^{II}, or Rh^{III} ions. The effect of metal-ion binding at this position on the properties of the nucleobase has been investigated, using experimental and theoretical methods.

Experimental Section

NMR spectra were measured on a JEOL model Lambda 500 spectrometer. Elemental analysis was performed using Carlo Erba model 1106 equipment. Mass spectroscopy was performed at the EPSRC National Mass Spectrometer Service Centre, University of Wales, Swansea, U.K. All reagents were purchased from Sigma−Aldrich, except for the metal salts, which were on loan from Johnson Mathey plc. 1-(N9-Adenine)-3,6-dithia-nonane-(*N1*-thymine) (**L3**) was prepared as previously described.[40] Ethylenediamine-*N*,9-ethyladenine (**L4**) was prepared by the previously reported method for the corresponding propyl analogue.[33]

N9-(2-Chloroethyl)adenine. To adenine (27 g, 200 mmol) and sodium hydride (60% dispersion in oil, 10 g, 250 mmol) in anhydrous dimethyl formamide (DMF) (500 mL) was added 1-bromo-2-chloroethane (36.0 mL, 430 mmol). The mixture was stirred under an atmosphere of nitrogen for 36 h. The resultant suspension was filtered through Celite. The solvent was removed from the filtrate under reduced pressure, and the crude product was recrystallized from ethanol (180 mL). This yielded the product as a white powder (8.6 g, 23%). ^{1}H NMR (d_6-DMSO): δ 4.09 (t, 2H, CH_2-CH_2-Ade), 4.59 (t, 2H, $Cl-CH_2-CH_2$), 7.31 (s, 2H, Ade-NH_2), 8.18 (s, 1H, C^2-H), 8.19 (s, 1H, C^8-H). Anal. Calcd for $C_7H_8ClN_5$: C, 42.63; H, 4.09; N, 35.53.

N9-(3-Chloropropyl)adenine. To a suspension of adenine (27 g, 200 mmol) and NaH (60% dispersion in oil, 10 g, 250 mmol) in dry DMF (500 mL) was added 1-bromo-3-chloropropane (22 mL, 220 mmol). The mixture was stirred under an atmosphere of nitrogen for 18 h. The suspension was filtered (Celite), and the filtrate was concentrated to a minimum volume under reduced pressure. Water (300 mL) was added and the mixture was extracted into chloroform (three times, 800 mL). The organic extracts were dried over $MgSO_4$. The solvent was removed, and the crude product was recrystallized from ethanol (180 mL) to give the product as a white microcrystalline solid (7.38 g, 17.43%). ^{1}H NMR (d_6-DMSO): δ 2.33 (m, 2H, $CH_2-CH_2-CH_2$), 3.65 (t, 2H, $Cl-CH_2-CH_2$), 4.29 (t, 2H, CH_2-CH_2-Ade), 7.30 (s, 2H, Ade-NH_2), 8.15 (s, 2H, C^2-H, C^8-H).

1-(N9-Adenine)-3,6-dithia-heptane, L1. To a solution of 1,2-ethanedithiol (0.48 g, 0.42 mL, 5.06 mmol) in dry DMF (100 mL)

(16) Suggs, W.; Dube, M. J.; Nichols, M. *Chem. Commun.* **1993**, 307.
(17) Young, M. A.; Jayaram, B.; Beveridge, D. L. *J. Am. Chem. Soc.* **1997**, *119*, 59.
(18) Hud, N. V.; Fiegon, J. *J. Am. Chem. Soc.* **1997**, *119*, 5756.
(19) Kickham, J. E.; Loeb, S. J.; Murphy, S. L. *Chem.—Eur. J.* **1997**, *3*, 1203.
(20) Meiser, C.; Song, B.; Freisinger, E.; Peilert, M.; Sigel, H.; Lippert, B. *Chem.—Eur. J.* **1997**, *3*, 388.
(21) Pearson, C.; Beauchamp, A. L. *Inorg. Chem.* **1998**, *37*, 1242.
(22) Tereshko, V.; Minasov, G.; Egli, M. *J. Am. Chem. Soc.* **1999**, *121*, 3590.
(23) Lan, T.; McLaughlin, L. W. *J. Am. Chem. Soc.* **2000**, *122*, 6512.
(24) Hamelberg, D.; McFail-Isom, L.; Dean Williams, L.; Wilson, W. D. *J. Am. Chem. Soc.* **2000**, *122*, 10513.
(25) Tereshko, V.; Wilds, C. J.; Minasov, G.; Prakash, T. P.; Maier, M. A.; Howard, A.; Wawrzak, Z.; Manoharan, M.; Egli, M. *Nucleic Acids Res.* **2001**, *29*, 1208.
(26) Kikuta, E.; Murata, M.; Katsube, N.; Koike, T.; Kimura, E. *J. Am. Chem. Soc.* **1999**, *121*, 5426.
(27) Houlton, A. *Adv. Inorg. Chem.* **2003**, *53*, 87.
(28) Mahnken, R. E.; Billadeau, M. A.; Nikonowicz, E. P.; Morrison, H. *J. Am. Chem. Soc.* **1992**, *114*, 9253.
(29) Lui, Y.; Pacifico, C.; Natile, G.; Sletten, E. *Angew. Chem., Int. Ed.* **2001**, *40*, 1226.
(30) Sheldrick, W. S.; Gunter, B. *J. Organomet. Chem.* **1989**, *375*, 233.
(31) Sheldrick, W. S.; Gunter, B. *J. Organomet. Chem.* **1991**, *402*, 265.
(32) Kickham, J. E.; Loeb, S. J.; Murphy, S. L. *J. Am. Chem. Soc.* **1993**, *115*, 7031.
(33) Price, C.; Elsegood, M. R. J.; Clegg, W.; Houlton, A. *J. Chem. Soc., Chem. Commun.* **1995**, 2285.
(34) Price, C.; Elsegood, M. R. J.; Clegg, M.; Rees, N. H.; Houlton, A. *Angew. Chem., Int. Ed. Engl.* **1997**, *36*, 1762.
(35) Shipman, M. A.; Price, C.; Elsegood, M. R. J.; Clegg, W.; Houlton, A. *Angew. Chem., Int. Ed.* **2000**, *39*, 2360.
(36) Shipman, M. A.; Price, C.; Gibson, A. E.; Elsegood, M. R. J.; Clegg, W.; Houlton, A. *Chem.—Eur. J.* **2000**, *6*, 4371.
(37) Price, C.; Shipman, M. A.; Rees, N. H.; Elsegood, M. R. J.; Edwards, A. J.; Clegg, W.; Houlton, A. *Chem.—Eur. J.* **2001**, *7*, 1194.
(38) Price, C.; Shipman, M. A.; Gummerson, S. L.; Houlton, A.; Clegg, W.; Elsegood, M. R. J. *J. Chem. Soc., Dalton Trans.* **2001**, 353.
(39) Gibson, A. E.; Price, C.; Clegg, W.; Houlton, A. *J. Chem. Soc., Dalton Trans.* **2002**, 131.
(40) Price, C.; Mayeux, A.; Horrocks, B. R.; Clegg, W.; Houlton, A. *Angew. Chem., Int. Ed.* **2002**, *41*, 1089.

was added NaH (0.12 g, 5.06 mmol), and the mixture was stirred until hydrogen evolution ceased. Iodomethane (MeI) (0.72 g, 0.32 mL, 5.06 mmol) was added, and the mixture was allowed to stir. After 16 h, a second equivalent of NaH was added (0.12 g, 5.06 mmol), and, again, the mixture was stirred until H_2 evolution was no longer observed. A solution of 9-(2-chloroethyl)adenine (1.00 g, 5.06 mmol) in dry DMF (100 mL) was added, and the suspension was stirred for an additional 16 h. The solution was filtered (Celite) and taken to dryness under reduced pressure; 100 mL of water was added, and the slurry was extracted into dichloromethane (three times, 300 mL). The organic extracts were dried (using Na_2SO_4). After evaporative removal of the solvent, the crude product was purified by column chromatography (packed with matrix 60 silica), eluting with a 15% mixture of EtOH in dichloromethane. Yield: 31%, 0.420 g. ^{1}H NMR (d_6-DMSO, δ, ppm, TMS): 2.15 (s, 3H, H16), 2.68 (t, 2H, H14), 2.75 (t, 2H, H13), 3.08 (t, 2H, H11), 4.41 (t, 2H, H10), 7.28 (s (br), 2H, H6), 8.20 (s, 1H, H2), 8.23 (s, 1H, H8). MS: 270, M + H. Anal. Calcd for $C_{10}H_{15}N_5S_2$: C, 44.59; H, 5.61; N, 26.0. Found: C, 45.57; H, 5.71; N, 25.57. A crystalline sample, suitable for analysis by single-crystal X-ray crystallography, was obtained from an aqueous solution adjusted to pH 1.5 by the addition of HNO_3.

1-(N9-Adenine)-4,7-dithia-octane, L2. The same procedure as that for 1-(N9-adenine)-3,6-dithia-heptane was used to synthesize 1-(N9-adenine)-4,7-dithia-octane (**L2**), with 9-(2-chloroethyl)adenine being replaced by 9-(3-chloropropyl)adenine. Yield: 34%, 0.461 g. ^{1}H NMR (d_6-DMSO, δ, ppm, TMS): 2.06 (s, 3H, H17), 2.09 (m, 2H, H11), 2.51 (t, 2H, H12), 2.55 (t, 2H, H14), 2.62 (t, 2H, H15), 4.22 (t, 2H, H10), 7.22 (s (br), 2H, H6), 8.14 (s, 2H, H2, H8). MS: 284, M + H. Anal. Calcd for $C_{11}H_{17}N_5S_2$: C, 46.61; H, 6.04; N, 24.70: Found: C, 45.82; H, 5.87; N, 24.71.

1-(N9-Adenine)-3,6-dithia-9-(N1-thymine)nonane, L3. Synthesis was as described elsewhere.[40]

[PdClL1]BF_4, 1. To a refluxing solution of $PdCl_2$ (0.038 g, 0.21 mmol) in acetonitrile (MeCN) (10 mL) was added dropwise a methanolic solution (10 mL) of ligand A-EtSSMe (0.057 g, 0.21 mmol); the mixture was refluxed overnight. The cooled solution was taken to dryness under reduced pressure, and the resultant solid residue was dissolved in hot water (50 mL); the mixture was filtered to remove any undissolved solids and concentrated to a minimum volume in vacuo. The addition of a saturated aqueous solution of $NaBF_4$ precipitated the product, which was washed with water, ethanol, and ether and then pump-dried. Yield: 53%, 0.057 g. Crystals suitable for single-crystal X-ray diffraction (XRD) studies were grown by controlled cooling of a hot aqueous solution. ^{1}H NMR (d_6-DMSO, δ, ppm, TMS): 2.68, 2.95 (s, 3H, H16), 3.41 (m, 1H, H14′), 3.56 (m, 3H, H13, H13′, H11′), 3.87 (m, 1H, H11), 3.89 (m, 1H, H14), 5.08 (m, 1H, H10′), 5.20 (m, 1H, H10), 8.32 (s, 1H, H8), 8.42 (s, 1H, H2), 8.45 (s (br) H6), 8.52 (s (br), 1H, H6′). ESMS: M^+, 411.9. Anal. Calcd for $C_{10}H_{15}BClF_4N_5PdS_2$: C, 23.69; H, 3.18; N, 13.81. Found: C, 23.89; H, 2.81; N, 13.81.

[PtClL1]BF_4, 2. To a refluxing aqueous solution of K_2PtCl_4 (0.08 g, 0.19 mmol in 30 mL) was added dropwise a methanolic solution (30 mL) of A-EtSSMe (0.052 g, 0.19 mmol), and the reaction was refluxed overnight. After cooling and concentration, a solid was isolated and redissolved in a minimum volume of cold water. The addition of a saturated solution of $NaBF_4$ gave the product as the BF_4 salt, which was washed with ethanol and ether and then pump-dried. Yield: 86%, 0.1 g. Single crystals suitable for X-ray analysis were grown by slow cooling of a hot aqueous solution. ^{1}H NMR (500 MHz, d_6-DMSO): δ 2.61, 2.93 (s, 3H, H16), 3.11, 3.16 (m, 1H, H13), 3.31 (m, 1H, H11), 3.35 (m, 1H, H14), 3.48 (m, 1H, H14′), 3.52 (m, 1H, H13′), 3.63, 3.79 (m, 1H, H11′), 4.72, 4.82 (m, 1H, H10), 5.10, 5.17 (m, 1H, H10′), 8.23 (s, 1H, H8), 8.37 (s, 1H, H2), 8.42 (s (br), 1H, H6), 8.456 (s (br), 1H, H6′). ^{195}Pt NMR (d_6-DMSO, δ, ppm): −1998.7, −2018.7 (ratio 2:1). Anal. Calcd for $C_{10}H_{15}BClF_4N_5PtS_2\cdot H_2O$: C, 19.86; H, 2.83; N, 11.58. Found: C, 19.74; H, 2.31; N, 11.39. MS (*m*/*z*): 500 M^+.

[PtClL2]BF_4, 3. K_2PtCl_4 (0.11 g, 0.27 mmol) was dissolved in distilled water (30 mL) and brought to reflux. A methanolic solution (30 mL) of A-PropSSMe (0.075 g, 0.27 mmol) was added dropwise to the hot solution. The reaction was kept at reflux ovenight. The solution was taken to dryness, and the remaining solid was dissolved in a minimum volume of cold water. An aqueous solution of $NaBF_4$ was added with stirring, and the resulting solid precipitate was collected by filtration. The product was washed sparingly with water, followed by ethanol and ether, and air-dried (0.112 g, 70%). ^{1}H NMR (d_6-DMSO, δ, ppm, TMS): 2.54 (m, 3H, H11′, H11, H12′), 2.76, 2.79 (s, 3H, H17), 3.01 (m, 1H, H14′), 3.16 (d, 1H, H15′), 3.30 (m, 1H, H15), 3.39 (m, 2H, H14, H12), 4.92, 4.95 (m, 1H, H10′), 6.32, 6.44 (m, 1H, H10), 8.36 (s, 1H, H8), 8.37 (s (br), 1H, H6), 8.39 (s, 1H, H2), 8.47 (s (br), 1H, H6). ^{195}Pt NMR (d_6-DMSO, δ, ppm, TMS): −1995.3, −2017.4 (2:1). MS (*m*/*z*): 514 M^+. Anal. Calcd for $C_{11}H_{19}BClF_4N_5OPtS_2$: C, 18.66; H, 2.37; N, 9.70. Found: C, 18.17; H, 2.49; N, 9.40.

[*mer*-$RhCl_3$L4], 4. $RhCl_3\cdot 3H_2O$ (0.34 g, 1.3 mmol) was dissolved in MeCN (50 mol) with heating. To this mixture was added dropwise an aqueous solution of A-Et-enH·Cl (0.34 g, 1.3 mmol in 25 mL). The solution was heated under reflux for 12 h, and the resulting solution was cooled to 4 °C. The resulting crystals were isolated by filtration. Yield: 18%, 0.1 g. ^{1}H NMR (d_6-DMSO, δ, ppm, TMS): δ 2.66 (m, 1H, H13), 2.80 (m, 2H, H14, H14′), 2.86 (m, 1H, H13′), 3.03 (m, 1H, H11), 3.16 (M, 1H, H11′), 4.32 (m, 1H, H10), 5.45 (m, 2H, H10′, H12), 5.69 (s (br), 1H, H15), 6.27 (s (br), 1H, H15′) 7.87 (s (br), 2H, H6, H6′), 8.12 (s, 1H, H8), 8.93 (s, 1H, H2). MS *m*/*z*: 394 = $[RhCl_2\mathbf{L}]^+$. Anal. Calcd for $C_9H_{15}N_7RhCl_3$: C, 25.11; H, 3.51; N, 22.77. Found: C, 24.78; H, 3.19; N, 21.83. Crystals suitable for X-ray analysis were grown from an MeCN:water mixture over a period of weeks.

[*mer*-$RhCl_3$L1], 5. $RhCl_3\cdot 3H_2O$ (0.19 g, 0.74 mmol) was dissolved in MeCN (30 mol) with heating. To this mixture was added, dropwise, a methanolic solution (30 mL) of A-Et-SS (0.19 g, 0.74 mmol). A color change from red to orange was noted after ∼1 h. The solution was heated under reflux for an additional 12 h, and the resulting solution was concentrated and cooled to 4 °C. The resulting solid was collected by filtration (0.05 g, 12%). ^{1}H NMR (d_7-DMF, δ, ppm, TMS): δ 2.44, 2.61 (s, 3H, H16), 3.22 (m, 1H, H13), 3.33 (m, 1H, H14), 3.50 (m, 2H, H11, H14′), 3.60 (m, 1H, H13′), 3.71 (m, 1H, H11′), 4.87, 4.92 (m, 1H, H10), 5.87, 5.95 (m, 1H, H10′), 8.21 (s, 2H, H6), 8.31, 8.32 (s, 1H, H8), 9.48, 9.54 (s, 1H, H2). MS *m*/*z*: 442 $[RhCl_2L]^+$. Anal. Calcd for $C_{10}H_{15}N_5RhS_2Cl_3$: C, 25.14; H, 3.16; N, 14.65. Found: C, 25.75; H, 3.03; N, 14.22. Crystals suitable for X-ray analysis were grown from a DMF:water mixture over a period of weeks.

X-ray Crystallography. All data were collected on Siemens−Bruker SMART CCD diffractometers. For the very small crystals of **3** and **4**, station 9.8 of the Synchrotron Radiation Source at Daresbury Laboratory was used, with wavelengths of 0.6942 and 0.6884 Å, respectively; Mo Kα radiation (λ = 0.71073 Å) was used for the other experiments. Crystal data and other experimental information are given in Table 1, with further details in the Supporting Information. Absorption corrections were applied by a semiempirical method, based on equivalent and repeated reflections in the data sets.[41] The structures were solved variously by direct and heavy-atom methods and refined on all unique F^2 values.[42] Disorder was resolved for the anions of **1** and **2** and for the MeCN

Table 1. Crystal Data and Experimental Information Regarding Various Complexes

property	[**L1**H]NO_3	**1**·0.5H_2O	**2**·0.5H_2O	**3**·H_2O	**4**·MeCN·H_2O	**5**·2DMF
formula	$C_{10}H_{16}N_5S_2{\cdot}NO_3$	$C_{10}H_{15}ClN_5PdS_2{\cdot}BF_4{\cdot}0.5H_2O$	$C_{10}H_{15}ClN_5PtS_2{\cdot}BF_4{\cdot}0.5H_2O$	$C_{11}H_{17}ClN_5PtS_2{\cdot}BF_4{\cdot}H_2O$	$C_9H_{15}Cl_3N_7Rh{\cdot}C_2H_3N{\cdot}H_2O$	$C_{10}H_{15}Cl_3N_5RhS_2{\cdot}2C_3H_7NO$
fw	332.4	507.1	595.8	618.8	489.6	624.8
cryst syst	monoclinic	monoclinic	monoclinic	monoclinic	monoclinic	monoclinic
space group	$P2_1/n$	$P2_1/c$	$P2_1/c$	$P2_1/c$	$C2/c$	$P2_1/n$
a (Å)	10.2207(14)	13.3530(11)	13.2833(11)	14.5324(12)	21.5759(12)	15.9976(9)
b (Å)	5.0621(7)	30.641(3)	30.410(3)	7.9967(7)	8.5451(5)	8.6960(5)
c (Å)	28.080(4)	8.5451(7)	8.5297(7)	16.4838(14)	19.8703(11)	18.8943(11)
β (deg)	95.719(2)	90.116(2)	90.188(2)	102.192(2)	98.266(2)	109.213(2)
V (Å^3)	1445.6(3)	3496.2(5)	3445.6(5)	1872.4(3)	3625.4(4)	2482.1(2)
Z	4	8	8	4	8	4
reflns measd	9633	25 301	26 670	9109	12 752	16 939
unique data, R_{int}	2524, 0.078	8316, 0.048	6772, 0.108	4900, 0.021	5027, 0.030	4364, 0.025
params	191	483	463	236	233	285
R (F, $F^2 > 2\sigma$)	0.064	0.039	0.080	0.032	0.030	0.035
R_w (F^2, all data)	0.169	0.076	0.193	0.078	0.090	0.077
GOF on F^2	1.09	1.01	1.08	1.17	1.05	1.18
max, min electron density (e/Å^3)	0.56, −0.47	0.88, −1.11	3.04, −2.78	1.62, −1.21	1.69, −0.73	1.78, −0.81

solvent in **4** and was refined with the aid of restraints. H atoms were constrained (but were not included for water and MeCN solvent molecules). The structures of **1** and **2** were found to be twinned by pseudo-merohedry, because of the closeness of the monoclinic β angle to 90°; the fractions of two twin components were refined satisfactorily in each case. The main residual electron density peaks were close to heavy atoms and disordered groups in each structure.

Calculations. All calculations were performed using the PC TITAN Version 1.05 molecular modeling package running on a Dell Precision 330 personal computer. Geometries were optimized using the Becke−Perdew density functional model, using an LACVP* basis set.

Cambridge Structural Database. For the analysis of alkyladenine derivatives, the Cambridge Structural Database (CSD) Version 5.22 was used with the following constraints: 3D-coordinated, $R < 0.05$, no disorder, no error, no polymer, no ions, organic.

Results and Discussion

Ligand and Complex Synthesis. Preliminary complexation reactions with the Pd^{II} ion and the mono-thiol **L**, prepared by the alkylation of 1,2-dithioethane with chloroethyladenine, gave a mixture of products that were not easily separated. The conversion of **L** to a thioether analogue (e.g., **L1**) allowed well-defined complexes to be isolated.

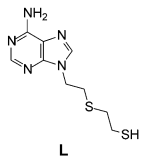

L

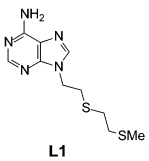

L1

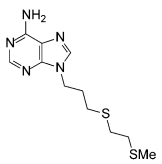

L2

The dithioether−adenine derivatives, **L1** and **L2**, were prepared by the stepwise deprotonation/alkylation of ethanedithiol. Deprotonation using NaH was followed by stoichiometric addition of MeI or the appropriate chloroalkyladenine. The workup in all cases involved chromatography over silica, with moderate yields obtained (∼30%). The compounds are soluble in DMSO, DMF, and methanol; however, they are not appreciably soluble in water at neutral pH. The ability to isolate the compounds as neutral molecules contrasts with the previously prepared diamine derivatives, which were isolated as hydrochloride salts.[33−38] In our hands, efforts to neutralize the latter compounds led to a loss of the ethylenediamine group.

The same stepwise procedure was used to prepare the self-complementary adenine−thymine (A−T)-containing thioether, **L3**, although in this case, N9-(2-chloroethyl)adenine was the initial alkylating agent, followed by 1-(3-chloropropyl)-thymine.[40] This sequence is necessary, because NaH will readily deprotonate T−N3 and increase its susceptibility to alkylation. The higher pK_a value of the exocyclic amino protons on A−N6 ensures that the second deprotonation step occurs preferentially at the thiol group.

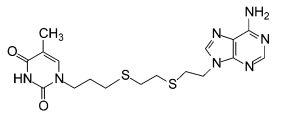

L3

For the synthesis of the Pd complex, **1**, $PdCl_2(MeCN)_2$ was generated in situ by refluxing $PdCl_2$ in MeCN and the dithioether ligand strand **L1** was added in methanol. As an aid to crystallization, the crude chloride salt was converted to the BF_4^- compound by metathesis in water, to give [PdCl**L1**]BF_4, **1**, as a yellow solid. The same procedure was used to prepare [PdCl**L3**]BF_4.[40]

The Pt complexes, [PtCl**L1**]BF_4 (**2**) and [PtCl**L2**]BF_4 (**3**), were prepared by the addition of a methanolic solution of the appropriate ligand to a refluxing aqueous solution of K_2PtCl_4. The as-prepared chloride salts were converted to the corresponding BF_4^- salts by metathesis in water, to give white solids. This was, again, done to facilitate crystallization and the compounds, as BF_4^- salts, were soluble in water, DMSO, and DMF.

The Rh complexes were prepared by adding the appropriate ligand, dissolved in water, in the case of **L4**, or methanol for **L1**, to a refluxing MeCN solution of $RhCl_3$. Orange

(41) Sheldrick, G. M. SADABS, Area Detector Absorption Correction Program; University of Göttingen: Germany, 1997.
(42) Sheldrick, G. M. SHELXTL, Version 5; Bruker AXS Inc., Madison, WI, 1997.

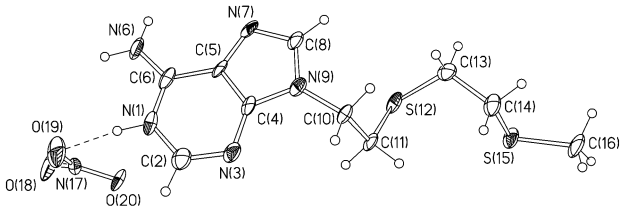

Figure 1. Cation and anion in [**L1**H](NO_3), with 50% probability displacement ellipsoids and atom labeling. The hydrogen bond between protonated N1 and nitrate is shown as a dashed line.

crystalline samples of [$RhCl_3$**L4**] (**4**) and [$RhCl_3$**L1**] (**5**) suitable for analysis by crystallographic methods were obtained in low yield (12%−18%) from mixed solvent systems by storage at low temperature for a period of several weeks.

Structural Studies. Single-crystal XRD analysis (Table 1) was used to establish the structural nature of the compounds definitively and to provide details of intermolecular interactions. Selected interatomic distances and angles are presented in Tables 2 and 3.

Thioether Ligand Strand. A crystalline sample of **L1** was isolated from an aqueous solution acidified with dilute HNO_3 (pH 1.2). In addition to confirming the nature of the compound (Figure 1), the quality of the X-ray data enables N1 to be identified as the site of protonation of the adenine. This is expected, on the basis of experimental and calculated literature data.[20] The significant structural change induced by protonation is a shortening of the C6−N6 bond length, which is 1.314 Å in **L1**, compared to that in alkyladenine derivatives in general (the average bond length is 1.337 Å for X-ray crystal structures in the CSD).[43] In the crystal lattice, the adeninyl groups self-pair through a Hoogsteen−Hoogsteen edge interaction (N6···N7 distance of 2.939 Å) and these pairs are arranged in a herringbone manner throughout the solid. The nitrate anions are hydrogen-bonded to N1 and N6.

Square Planar Complexes. The crystal structure of the Pd complex, **1**, contains two independent cations that differ primarily in the orientation of the terminal S-Me group, together with BF_4^- anions and water molecules. The complex cations, [PdCl**L1**]$^+$, exhibit a distorted square planar structure that is shown in Figure 2, and Table 2 gives interatomic distances and angles. **L1** acts as a tridentate ligand, with the two S atoms and N3 of adenine being involved in binding the metal ion. A chloride ion occupies the remaining coordination site. The dihedral angles between the adenine moiety and the coordination plane (defined by Pd1/N3/S12/S15/Cl1) are 49.5° and 48.6° for the two molecules. Compared to the ethylenediamine analogue, [PdCl**L4**]$^+$,[37] the effect of the thioether S-donor trans to the N3 does not significantly affect the Pd−N3 bond lengths (2.070/2.078 Å versus 2.047 Å).

The Pt complexes, [PtCl**L1**]BF_4 (**2**) and [PtCl**L2**]BF_4 (**3**), are similar to the Pd complex **1**, and, as expected, the complex cations exhibit distorted square planar geometries. In fact, **2** is isostructural with the Pd complex **1**, with two

(43) Allen, F. H.; Kennard, O. *Chem. Des. Autom. News* **1993**, *8*, 31.

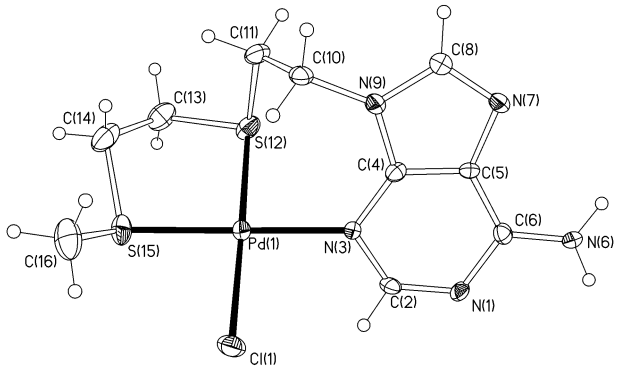

Figure 2. One of the two independent [PdCl**L1**]$^+$ cations in **2**·0.5H_2O, with 50% probability displacement ellipsoids. The other cation (with atom names ending in A) has essentially the same structure. The analogous Pt complex **3**·0.5H_2O is isostructural.

Table 2. Selected Bond Lengths (Å) and Angles (deg) for the Square Planar N3-Bound Adenine Complexes **1**, **2**, and **3**[a]

	1 (M = Pd)	**2** (M = Pt)	**3** (M = Pt)
M(1)−N(3)	2.069(4)	2.058(16)	2.056(4)
	2.079(4)	2.049(15)	
M(1)−S(12) or M(1)−S(13)	2.2864(14)	2.260(5)	2.2551(12)
	2.2815(13)	2.261(4)	
M(1)−S(15) or M(1)−S(16)	2.2702(13)	2.257(5)	2.2622(11)
	2.2803(13)	2.261(5)	
M(1)−Cl(1)	2.3103(12)	2.311(4)	2.3113(12)
	2.3153(12)	2.307(4)	
N(6)−C(6)	1.324(6)	1.31(2)	1.322(6)
	1.325(6)	1.33(2)	
H[C(10)]···M(1)	2.768	2.836	2.588
	2.702	2.650	
dihedral angle between nucleobase	49.6	49.1	72.3
and ligand coordination plane	48.8	49.7	

[a] Two independent molecules were in the unit cell for complexes **1** and **2**.

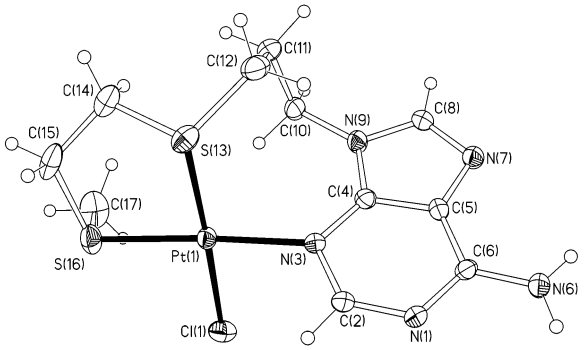

Figure 3. [PtCl**L2**]$^+$ cation in **3**·H_2O, with 50% probability displacement ellipsoids.

independent molecules in the unit cell. Table 2 includes interatomic distances and angles for **2** and **3**, and Figure 3 shows the complex cation in **3**. Replacing the Pd^{II} ions with Pt^{II} ions has little effect on the metal−ligand bond lengths. A striking difference between the structure of **3** compared to those of **1** and **2** is the dihedral angle between the adenine moiety and the coordination plane. The extra methylene group in the propyl ligand **L2** of **3** allows the adenine to adopt an orientation that is more typical of simple alkylated nucleobases in complexes (the range of observed dihedral angles is 61°−82° for simple complexes;[20] cf. 72.3° in **3** and 48.6°, 49.5° in **1** and **2**). The N9-bound ethyl chain of **L1** forces smaller values for this angle.

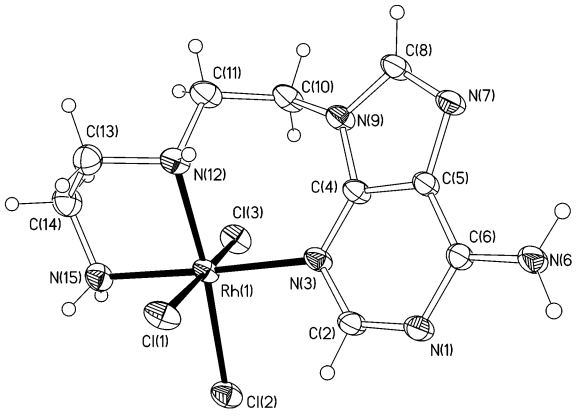

Figure 4. $[RhCl_3\mathbf{L4}]^+$ cation in **4**·MeCN, with 50% probability displacement ellipsoids.

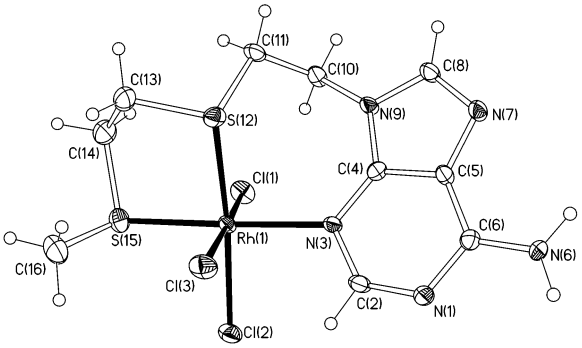

Figure 5. $[RhCl_3\mathbf{L1}]^+$ cation in **4**·2DMF, with 50% probability displacement ellipsoids.

Table 3. Selected Bond Lengths (Å) and Angles (deg) for the Octahedral N3-Bound Adenine Complexes **4** and **5**

	4	**5**
Rh(1)−N(3)	2.098(2)	2.129(3)
Rh(1)−N(12) or Rh(1)−S(12)	2.067(2)	2.3064(9)
Rh(1)−N(15) or Rh(1)−S(15)	2.033(2)	2.3036(10)
Rh(1)−Cl(1)	2.3598(6)	2.3546(9)
Rh(1)−Cl(2)	2.3590(7)	2.3688(9)
Rh(1)−Cl(3)	2.3216(6)	2.3366(8)
N(6)−C(6)	1.331(3)	1.327(4)
H[C(10)]···Rh(1)	3.171	3.219
dihedral angle between nucleobase and ligand coordination plane	34.5	37.8

In all three complexes, the folding of the thioalkyl chain locates one of the protons of the N9-bound methylene (C10) in an apical site above the metal ion. This can be seen particularly for the cation **3** (Figure 3). The short M···H distance is in the range of 2.59−2.84 Å (with uncorrected constrained C−H bond lengths of 0.99 Å, appropriate for XRD), sufficiently short to be considered as an agostic interaction.[37] The effect of this close proximity between the metal ion and the ligand protons is seen as a large downfield shift in the ^{1}H NMR spectra (vide infra).

Octahedral Complexes. Figures 4 and 5 show the molecular structures of the Rh^{III} complexes $[RhCl_3\mathbf{L4}]$ (**4**) and $[RhCl_3\mathbf{L1}]$ (**5**), and selected distances and angles are given in Table 3. In both complexes, the chelate-tethered adenine adopts the same type of tridentate binding mode as seen in the square planar complexes **1**−**3**. Hence, the ligand strands bind in a mer-conformation. It was interesting to verify that these ligand systems are capable of coordinating an octahedral metal center via N3. Our previously reported octahedral complexes involved metal−C8 binding.[34,37] In these cases, the purine-ethyl-ethylenediamine group is in a coplanar conformation. However, binding via N3 requires the ligand strand to be significantly folded. The short M··· H[C(10)] distances caused by this folding might preclude N3 binding to an octahedral metal center, because of steric interactions with the axial ligands. In fact, the trans-chloro group in these complexes is accommodated by a reduction in the dihedral angle between the adenine moiety and the planes defined by (Rh/N3/N12/N13/Cl2) in **4** and (Rh/N3/S12/S15/Cl2) in **5** (34.5° in **4**; 37.8° in **5**). This conformational change increases the distance between the H10 protons and the metal center significantly, compared to that observed in the square planar complexes (3.17 Å for **4**, 3.22 Å for **5**).

Another point of interest is that the Rh^{III} ion lies some distance out of the adeninyl plane in both complexes (0.66 Å in **4**, 0.48 Å in **5**). For the square planar complexes reported here, the corresponding distances are much smaller (in the range of 0.02−0.20 Å). This greater displacement in the Rh complexes is likely to be the result of a mismatch between the constraints of the ligand conformation and the octahedral coordination geometry, rather than electronic factors.

To the best of our knowledge, no previous examples of N3-bound Rh^{III} complexes have been structurally characterized. Sheldrick and Gunter prepared and characterized N3-bound Rh^{I} complexes of N9-benzyladenine[44] and 6,6′-dimethyladenine.[30,31] The Rh^{I}−N3 distances (in the range of 2.100−2.188 Å) are similar to the distances for the complexes reported here.

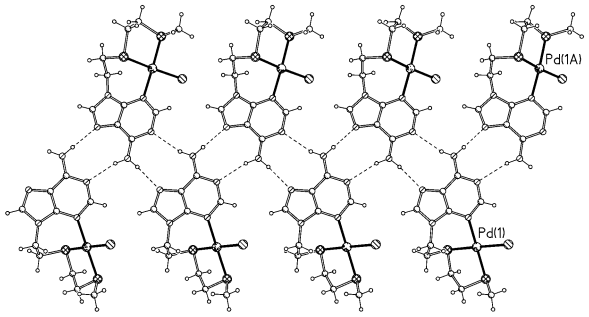

Figure 6. Section of the molecular packing for the cations of **1**, showing the conserved hydrogen-bonding motif, which involves interactions between the Watson−Crick and Hoogsteen faces of the coordinated adenines and generates metal-edged tapes with metal...metal separations of 8.545 Å (the unit cell *c*-axis length).

Crystal Packing. The molecular architecture of the crystal packing of all the compounds is remarkably similar. The predominant pattern involves a polar arrangement of adenine moieties interacting via Watson−Crick → Hoogsteen face hydrogen bonding (N1/HN6 → HN6/N7) to form a zigzag arrangement. Thus, tapes are formed that have the nucleobase on the inside and the metallo group on the outside edge (see Figures 6 and 7). These tapes are separated from anions and solvent molecules. In each case, the tapes run parallel to the shortest axis of the unit cell, and this axis length is the

(44) Sheldrick, W. S.; Gunter, B. *Inorg. Chim. Acta* **1988**, *152*, 223.

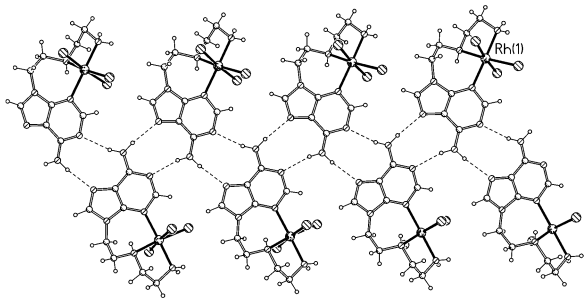

Figure 7. Section of the molecular packing for the cations of **4**, showing the conserved hydrogen-bonding motif. The metal-edged tapes here also have metal...metal separations of 8.545 Å (the unit cell *b*-axis length).

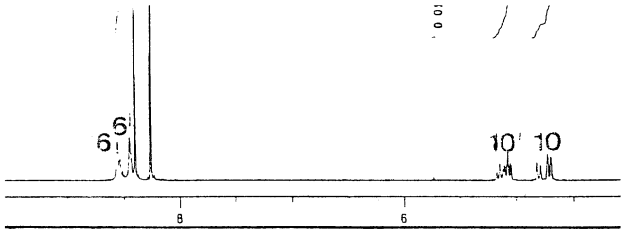

Figure 8. Downfield region of the ^{1}H NMR of **3** in d_6-DMSO highlighting the splitting of the N6-amino protons of the adeninyl group. Note also the two sets of resonances for the C10-methylene protons, which are due to slow inversion at the S atom.

metal...metal separation on the tape edge, ranging between 7.997 (for **3**) and 8.696 Å (for **5**). Interlayer interactions are somewhat modified, presumably by the presence of the extra chloro ligands in the octahedral Rh^{III} complexes and by the different solvent molecules.

Solution-State Analysis. The ^{1}H NMR spectra of the complexes **1**−**3** show the presence of two isomers in an ∼2:1 ratio, corresponding to syn and anti conformations arising from slow inversion at the terminal S-Me group. In keeping with this theme, the ^{195}Pt NMR spectra for **2** and **3** contain two resonances with the same 2:1 ratio. The shift values are δ −1999 and −2019 ppm (2:1) for **2** and δ −1995 and −2017 ppm (2:1) for **3**.

Complexes **1**−**3** show predominantly downfield shifts for the ligand protons, compared to the uncomplexed adenine derivative. For example, slight changes in the positions of H2 and H8 are seen, with H2 experiencing the larger shift (∼0.1 ppm). The methylene protons on C10 are significantly shifted, with the proton closest to the metal ion again being the most affected. The magnitude of the shifts is particularly pronounced for the propyl analogue **3** (cf. $\Delta\delta$ **1**, 0.59, 0.67 ppm; **2**, 0.31, 0.41, 0.69, 0.76 ppm; **3**, 0.70, 0.73, 2.10, 2.2 ppm). This complex has the shortest metal···H10 distance in **1**−**5** at 2.588 Å. For both Pt complexes, **2** and **3**, two resonances are observed for each of the H10 protons, indicating two chemically distinct environments.

The general trends in the NMR data for the square planar complexes are also observed in the octahedral Rh^{III} complexes. However, a much larger difference in the chemical shifts of the aromotic adenine protons is observed (Figure 8). In **4**, the H2 resonance is shifted far downfield, compared to that of H8 (δ H8 8.12; cf. H2 8.93 ppm). In the thioether analogue, **5**, the effect is even more extreme, and each

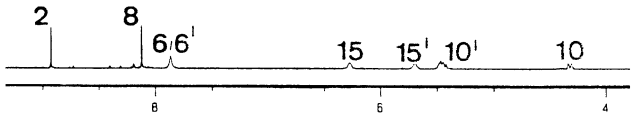

Figure 9. Downfield region of the ^{1}H NMR of **4** in d_6-DMSO. Note the absence of splitting of the N6-amino protons of the adeninyl group.

resonance is also split into two signals, because of the conformational isomers present (δ H8 8.31, 8.32 ppm; δ H2 9.48, 9.54 ppm).

Perhaps most dramatic is the effect of coordination on the exocyclic amino protons H_2N6. For the square planar complexes, a downfield shift of ∼1.1 ppm is seen in each case, compared to that of the uncomplexed adenine. Moreover, the single resonance observed in the free ligand is split into two in the complexes ($\Delta\delta$ **1**, +1.17, +1.24 ppm; $\Delta\delta$ **2**, 1.14, 1.28 ppm; $\Delta\delta$ **3**, 1.15, 1.25 ppm) (Figure 8). Similar shifts are also seen in the Rh complexes, with the largest in **5** at 1.93 ppm; however, the resonance is not split in either case (Figure 9).

A simple explanation for this observation is a restricted rotation about the N6−C6 bond, induced by an increase in resonance with the adeninyl aromatic core, because of metal-ion binding. Concomitant with this would be a shortening of the N6−C6 bond length and a planarization of the amino group. The crystal structure data for the metal complexes here show a narrow range of C6−N6 bond lengths, 1.322(6)−1.33(2) Å, and these are longer than those for the N1-protonated ligand, [**L1**H]$^+$. The previously reported Pd−N3-adenine-diamine derivatives have C6−N6 distances of 1.326(5) [PdCl-Ade-Et-en]$^+$ and 1.312(5) Å [PdCl-Ade-Prop-en]$^+$, respectively.[37] The lack of splitting for the H_2N group in the Rh complexes suggests a reduced ability to enhance this resonance, which may be related to the observed out-of-plane nature of the Rh−adeninyl bond.

An analysis of the CSD (Version 5.22) for alkyladenine derivatives shows a similar effect for protonation. An average C6−N6 distance of 1.337 Å with a range of 1.329−1.352 Å was found for nonprotonated compounds (33 structures). Surveying the database again, it was noted that the effect of N1 protonation was to shorten the N6−C6 distance (1.304−1.332 Å; average length of 1.3196 Å for seven structures). The C6−N6 distance in **L1** (1.314 Å) is very close to this average value, and it is significantly shorter than in the metal complexes. Further support for this bond shortening upon cation binding is seen in the electronic structure calculations (vide infra).

Effect of N3 Coordination on Adenine Basicity. The effect of metal-ion binding on the acid−base properties of DNA bases has been extensively investigated.[45−49] However, the difficulty in preparing mononuclear N3-coordinated

(45) Gunnar, K.; Kapinos, L. E.; Griesser, R.; Lippert, B.; Sigel, H. *J. Chem. Soc., Perkin Trans. 2* **2001**, 1320.
(46) Song, B.; Zhao, J.; Griesser, R.; Meiser, C.; Sigel, H.; Lippert, B. *Chem.—Eur. J.* **1999**, *5*, 2374.
(47) Sigel, H.; Song, B.; Oswald, G.; Lippert, B. *Chem.—Eur. J.* **1998**, *4*, 1053.
(48) Blindauer, C. A.; Emwas, A. H.; Holy, A.; Dvorakova, H.; Sletten, E.; Sigel, H. *Chem.—Eur. J.* **1997**, *3*, 1526.
(49) Sigel, H.; Song, B. *Met. Ions Biol. Syst.* **1996**, *32*, 135.

Table 4. Electrostatic-Potential Fitted Atomic Charges Calculated at the BP-LACVP* Level of Theory, and Selected Metrical Parameters

atom	9-MeA	9-MeA-N3H$^+$	*anti*-**2**	**4**	[PdCl(**L4**)]$^+$	[Pt(NH$_3$)$_3$(N3-9-MeA)]$^{2+}$	[PtCl(NH$_3$)$_2$(N3-9-MeA)]$^+$
N1[a]	−0.637	−0.497	−0.554	−0.548	−0.521	−0.492	−0.553
N3[a]	−0.615	−0.421	−0.260	−0.119	−0.188	−0.139	−0.126
N7[a]	−0.463	−0.417	−0.422	−0.454	−0.429	−0.431	−0.473
N6[a]	−0.763	−0.702	−0.750	−0.795	−0.729	−0.675	−0.759
H6a[a]	0.366	0.412	0.413	0.394	0.405	0.415	0.410
H6b[a]	0.361	0.402	0.394	0.385	0.388	0.398	0.397
H2[a]	0.052	0.142	0.107	0.126	0.120	0.079	0.104
H8[a]	0.124	0.166	0.161	0.134	0.150	0.162	0.156
M−N3 (Å)			2.073 (2.058)[b]	2.107 (2.098)[b]	2.052 (2.047)[b]	2.056	2.046
N6−C6 (Å)	1.365	1.335	1.344 (1.33)[b]	1.354 (1.331)[b]	1.345 (1.326(5))[b]	1.334	1.343
∑∠HNH (°)	353.2	360.0	360.0	360.0	359.9	360.0	359.8
absolute energy (kJ/mol)	−1 329 945	−1 330 937	−5 354 131	−5 842 471	−3 470 759	−2 087 157	−3 147 691

[a] Data given are calculated atomic charges. [b] Value given in parentheses is from the X-ray crystal structure data.

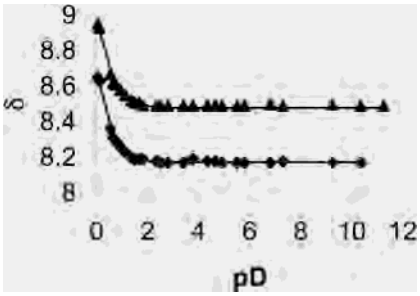

Figure 10. Plot of δ vs pD for the adeninyl protons (▲) H2 and (◆) H8 in complex **2**. The calculated pK_a value is -0.16 ± 0.26.

adenine derivatives has meant that this site has been more difficult to assess.[20] The compounds described here are useful in addressing such questions about both the acidity constant and the site of protonation of interest. These studies were restricted to the Pt^{II} complexes, because the Pd^{II}- and Rh^{III}-containing compounds are not sufficiently stable at low pH.

^{1}H NMR spectroscopy was used to determine the pK_a value for the Pt^{II} complex **2**. Figure 10 shows a plot of δ versus pD, and analysis of these data gives a pK_a value of -0.16 ± 0.26. This value is in agreement with that found for a Pt^{II} complex of 6,6,9-trimethyladenine [Pt(dien)(N3-6,6,9-TMAH-N1)]$^{3+}$, or 6,6,9-TMA) (pK_a = 0.3).[20] As expected, these values are significantly lower than the pK_a values of 4.2, 4.3, and 4.15 reported for the initial protonation of adenine, 9-methyladenine (9-MeA), and 6,6,9-TMA, respectively. In these cases, the initial site of protonation is N1.[20] Interestingly, Lippert and Sigel found that N3 coordination reverses the normal sequence of protonation site and, on the basis of NMR data, identified N7 as being the initial protonation site in [Pt(dien)(N3-TMA)]$^{2+}$.[20] As can be seen from Figure 8, no preferential shift in either the H2 or H8 resonances is evident, which makes an assignment of the site of protonation problematic. The data suggest that either (i) protonation is in rapid exchange at the two sites N1 and N7, or (ii) binding at one site (e.g., N1) produces a coincidentally equivalent effect on both H2 and H8. Unfortunately, all attempts to crystallize the metal complexes in protonated form were unsuccessful.

Effect of N3 Coordination on Base-Pair Hydrogen Bonding in L3. We have recently reported on the synthesis of self-complementary metal complexes that contain an N3-bound adenine and a pendant thymine group based on **L3**.[40] In the solid state, [PtCl**L3**][BF$_4$] contains complex cations interacting through Hoogsteen base pairs, the most thermodynamically stable permutations for an AT pair. The effects of coordination upon the solution-state interactions of the AT-containing ligand strand were investigated. The concentration dependence of the ^{1}H NMR spectra of the **L3** alone in d_6-DMSO gave evidence for weak self-association, with a calculated value for the association constant of $K = 0.64$ M^{-1}. This was supported by ESMS data for solutions of **L3** in methanol that showed evidence for association (m/z = 843 [**L3**$_2$ + H]; m/z = 865 [**L3**$_2$ + Na]). The association constant is much smaller than the value found for AT-anthracenyl derivatives (35 ± 5 M^{-1}) reported by Sessler, although, in this case, a mixed d_6-DMSO/CDCl$_3$ solvent system was used.[50] The lack of conformational rigidity in **L3** would also reduce the association process, compared to a more rigid system. By comparison, no shifts in ^{1}H NMR resonances are seen for [PtCl**L3**][BF$_4$] up to saturation concentrations (~250 mM).

The lack of self-association for the complex [PtCl**L3**]$^+$, compared to that for **L3** alone, suggests that either (i) the charge on the complex cations reduces the self-association, compared to the thioether stand, (ii) metal-ion binding at N3 reduces the ability to form a base pair with thymine, or (iii) a combination of both factors is involved. Point (ii) is in contrast to the effect of Pt^{II} binding to G−N7 (or C−N1) on guanine:cytosine (GC) base pairing,[5−7] in which the metal-ion coordination enhances the base-pairing interaction.

Electronic-Structure Calculations. In an effort to gain further insight into the effect of N3 coordination on the electronic structure of adenine, including identification of the probable site of protonation, a series of density functional calculations were perfomed. Calculations were at the BP-LACVP* level of theory for selected metal complexes, their protonated counterparts, and model 9-MeA derivatives. Details are summarized in Tables 4−6.

Comparison of the calculated structures reveals a shortening of the C6−N6 bond length in the sequence 9-MeA > **5** > **3** > 9-MeA-N3H$^+$ upon protonation/metal-ion binding at N3 (Table 4). The exocyclic amino group also becomes

(50) Sessler, J. L.; Wang, R. *J. Am. Chem. Soc.* **1996**, *118*, 9808.

Table 5. Protonation Energies for Alkyladenine Derivatives Calculated at the BP-LACVP* Level of Theory

compound	protonation energy (kJ/mol) absolute	relative
[9-MeA(N1H)]$^+$	−1 330 941	0
[9-MeA(N3H)]$^+$	−1 330 937	+4
[9-MeA(N7H)]$^+$	−1 330 916	+25
[9-MeA(N3,N1(H$_2$)]$^{2+}$	−1 331 468	+33
[9-MeA(N3,N7(H)$_2$]$^{2+}$	−1 331 501	0
[**2**(N1H)]$^{2+}$	−5 354 817	0
[**2**(N7H)]2+	−5 354 800	+17
[**4**(N1H)]$^+$	−5 843 412	0
[**4**(N7H)]$^+$	−5 843 366	+46
[PdCl(**L4**N1H)]$^{2+}$	−3 471 445	0
[PdCl(**L4**N7H)]$^{2+}$	−3 471 424	+21
[N3-PtCl(NH$_3$)$_2$-9-MeA(N1H)]$^{2+}$	−3 148 360	+13
[N3-PtCl(NH$_3$)$_2$-9-MeA(N7H)]$^{2+}$	−3 148 373	0
[N3-Pt(NH$_3$)$_3$-9-MeA(N1H)]$^{3+}$	−2 087 563	+20
[N3-Pt(NH$_3$)$_3$-9-MeA(N7H)]$^{3+}$	−2 087 583	0

planar. We have noted this effect previously for inner- and outer-sphere binding of group I metal ions to A−N3.[39] These structural changes are consistent with an increase in resonance between the NH_2 group and the purine core, which, if sufficient, would restrict the rotation about the C6−N6 bond. The ^{1}H NMR data indicate that the Pd^{II} and Pt^{II} (square planar) complexes are more effective in enhancing this than the Rh^{III} complex is, because, in the former cases, the resonance for this group is split. Although the bond length differences are small (1.354 Å for **5**, cf. 1.344 Å for **3**), it may be significant that the calculated structures are consistent with this observation.

The electrostatic atomic charges are perturbed upon coordination, with a decrease in the negative charge on the endocyclic nitrogen atoms N1, N3, and N7, which is consistent with the much-reduced pK_a value for the N3-coordinated adenine. Protonation has a similar, although larger, effect. A consistent finding is that N1 retains a higher negative charge than N7; however, the difference ($E_{Pot-N1} - E_{Pot-N7}$) is reduced. N3 binding affects the charge on the exocyclic amino protons, which becomes more positive, as expected for a more planar amino group.

A summary of the gas-phase calculated data on protonated adenine derivatives is given in Table 5. The calculations here are in broad agreement with the data of other workers.[51] For monoprotonated 9-MeA, the relative energy of the three possible species in the gas phase increases in the following order: H^+N1 < H^+N3 < H^+N7. For model compounds [Pt(NH$_3$)$_3$(N3-9-MeA-H-N1)]$^{3+}$ and [Pt(NH$_3$)$_3$(N3-9-MeA-H-N7)]$^{3+}$, the N7-protonated species is of lower energy (−20 kJ/mol). This ordering is also true for the pair of dicationic species [PtCl(NH$_3$)$_2$(N3-9-MeA-H-N1)]$^{2+}$ and [PtCl(NH$_3$)$_2$-(N3-9-MeA-H-N7)]$^{2+}$, although the difference is reduced (13 kJ/mol). These data support the switch in the preferred protonation site for N3-coordinated adenine derivatives, in agreement with the experimental results on 6,6,9-TMA complexes of Sigel and Lippert.[20]

It is somewhat surprising to then find that, for the chelate-tethered derivatives, regardless of the metal ion (Pd^{II}, Pt^{II}, or Rh^{III}), the more stable complex is the N1-protonated species. The difference between the two forms varies from 17 kJ/mol for the Pt^{II} complex **2**, to 46 kJ/mol for the Rh^{III} complex **4**.

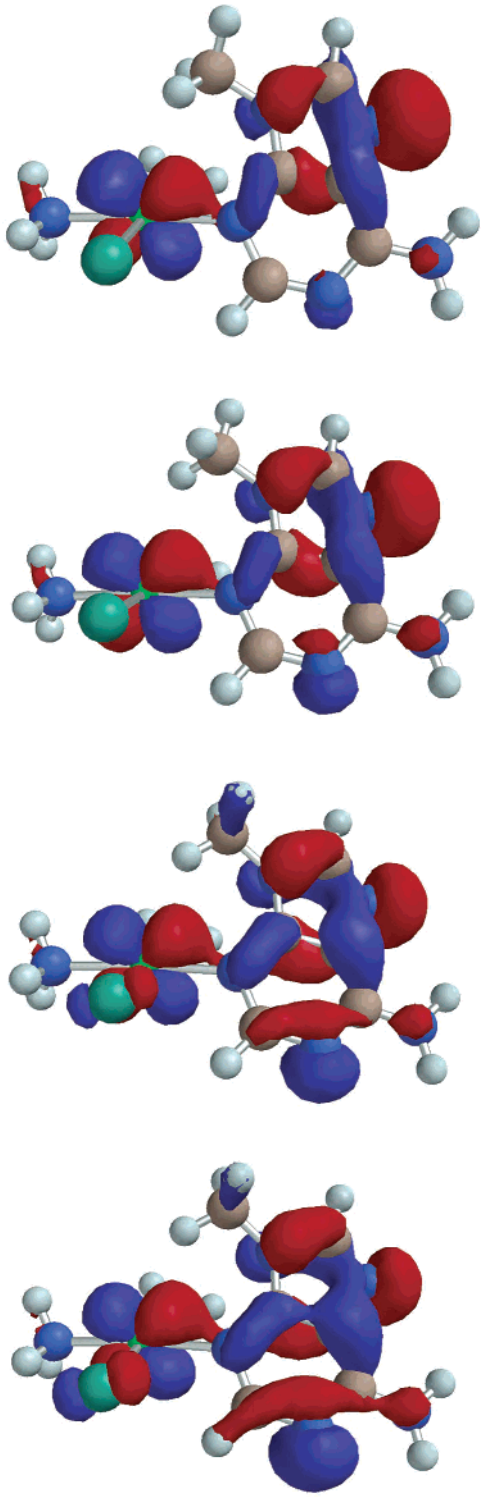

Figure 11. HOMO for [PtCl(NH$_3$)$_2$(N3-9-MeA)]$^{2+}$ calculated for fixed conformations. The molecules shown have, from top to bottom, angle α (as defined in Table 6) = 120°, 130°, 140°, and 150°, respectively. Note the increase in contribution from N1-based orbitals and a concomitant decrease from N7 as the adeninyl moiety is rotated increasingly toward the metal-ion coordination plane.

The most significant structural difference between **2** and the model compound [PtCl(NH$_3$)$_2$(N3-9-MeA)]$^+$ is the angle

(51) Šponer, J. E.; Leszczynski, J.; Glahe, F.; Lippert, B.; Šponer, J. *Inorg. Chem.* **2001**, *40*, 3269.

Table 6. Angle Dependence of the Protonation Energies for the Model Compound $[PtCl(NH_3)_2(N3\text{-}9\text{-}MeA)]^{+a}$

	equilibrium geometry	α = 120°	α = 130°	α = 140°	α = 145°	α = 150°
			$[PtCl(NH_3)_2(N3-9\text{-}MeA)]^+$			
absolute energy (kJ/mol)	−3 147 690 (α = 70°)	−3 147 676	−3 147 672	−3 147 668	−3 147 668	−3 147 693
			$[PtCl(NH_3)_2(N3-9\text{-}MeA\text{-}N1H)]^{2+}$			
absolute energy (kJ/mol)	−3 148 360 (α = 70°)	−3 148 380	−3 148 375	3 148 371	−3 148 341	−3 148 364
protonation energy (kJ/mol)	670.19	703.24	703.24	702.40	672.70	671.02
			$[PtCl(NH_3)_2(N3-9\text{-}MeA\text{-}N7H)]^{2+}$			
absolute energy (kJ/mol)	−3 148 373 (α = 56°)	−3 148 373	−3 148 367	−3 148 360	−3 148 330	−3 148 351
protonation energy (kJ/mol)	682.74	696.54	695.29	691.94	661.82	658.05
$E_{HN1} - E_{HN7}$ (kJ/mol)	−12.55	6.70	7.95	10.46	10.88	12.97

[a] Angle α is defined as the dihedral angle Cl−Pt−N3−C4, as shown in the scheme below. For equilibrium geometry, no constraints were imposed and the final angle α is quoted.

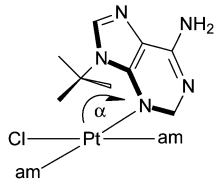

between the adenine group and the metal-ion coordination plane. This is due to restrictions imposed by the chelating tether, which prohibit a range of conformations otherwise available to the 9-MeA derivative. Hence, the angle dependence of protonation energies was investigated for the model compound $[PtCl(NH_3)_2(N3\text{-}9\text{-}MeA)]^+$, which is closely analogous to **2** but lacks the tether. Table 6 summarizes the data and shows that, for these molecules, as the adeninyl moiety is rotated toward the metal-ion coordination plane, there is a switch-over in the preferred proton binding site from N7, as observed by Sigel and Lippert,[20] to N1. The basis for this can be seen in Figure 11, which depicts the highest occupied molecular orbital (HOMO) of the model compound $[PtCl(NH_3)_2(N3\text{-}9\text{-}MeA)]^+$. As the adeninyl group is rotated toward the metal coordination plane, the contribution to the HOMO from N1 increases whereas, for N7, the orbital contribution decreases. The difference in energy between the most stable species in the two extreme geometries investigated is ∼25 kJ/mol. We are not aware of such effects being noted previously.

Conclusion

The attachment of a chelating tether to adenine allows the rational synthesis of N3-coordinated complexes. A wide range of metal-ion coordination geometries can be accommodated by these ligands, including square planar, square-based pyramidal, trigonal bipyramidal, and octahedral. In the solid state, compounds **1**−**5** crystallize with a conserved hydrogen-bonding motif that involves polar Watson−Crick → Hoogsteen interactions between adjacent adenine. Binding the Pt^{II} ion at A−N3 lowers the pK_a value from ∼4 to −0.16 ± 0.25, in agreement with other literature values.[20] Calculations at the BP-LACVP* level of theory indicate that N1 is retained as the initial site for protonation in these complexes; however, the N1/N7 preference is subtly balanced and shows conformational dependence. The base-pairing ability of the AT-containing ligand strand **L3** is also appears to be diminished by complexation.

Acknowledgment. The EPSRC is thanked for the award of grants to support M.A.S. and D.A., for an Advanced Research Fellowship to A.H., and for partial funding for a diffractometer (W.C.). The EPSRC MS Service Centre, University of Wales, Swansea, is also acknowledged. The BBSRC is thanked for the award of a grant to support C.P. Professor W. McFarlane is thanked for assistance with the NMR experiments. Johnson Mathey plc is thanked for the generous supply of metal salts.

Supporting Information Available: X-ray crystallographic data in CIF format, for complexes characterized herein. This material is available free of charge via the Internet at http://pubs.acs.org.

IC020657G